# Accepted Manuscript

New BN-epoxy composites obtained by thermal latent cationic curing with enhanced thermal conductivity

Isaac Isarn, Lluís Massagués, Xavier Ramis, Àngels Serra, Francesc Ferrando

**New BN-epoxy composites obtained by thermal latent cationic curing with enhanced thermal conductivity**

**Isaac Isarn[a], Lluís Massagués[b], Xavier Ramis[c], Àngels Serra[d], Francesc Ferrando[a]***

*a. Department of Mechanical Engineering, Universitat Rovira i Virgili, C/Av. Països Catalans, 26, 43007*

*Tarragona, Spain.* isaac.isarn@urv.cat, f.ferrando@urv.cat

*b. Department of Electronic, Electric and Automatic Engineering, Universitat Rovira i Virgili, C/Av.*

*Països Catalans, 26, 43007 Tarragona, Spain.* lluis.massagues@urv.cat

*c. Thermodynamics Laboratory, ETSEIB, Universitat Politècnica de Catalunya. C/Av. Diagonal 647,*

*08028 Barcelona, Spain.* ramis@mmt.upc.edu

*d. Department of Analytical and Organic Chemistry, Universitat Rovira i Virgili, C/ Marcel·lí Domingo*

*s/n, 43007 Tarragona, Spain.* angels.serra@urv.cat

\* To whom the correspondence should be addressed.

**Abstract**

A series of boron nitride (BN) composites, with different BN content, were prepared and characterized by cationic curing of DGEBA/BN formulations. As cationic initiator a commercial benzylanilinium salt was used. This cationic system shows good latent characteristics that were not lost on adding the filler. The performance of the catalytic system was optimized by varying the amount of initiator and adding little proportions of glycerol. The kinetics of the curing process was evaluated by calorimetric measurements. The addition of BN allowed increasing thermal conductivity without loss of mechanical properties like Young modulus, impact resistance, adhesion and other thermal characteristics like Tg or thermal stability. In addition, dielectric properties were improved with the increment of filler.

## 1. Introduction

The continuous trend of doing more with less is the tendency in our technological world and definitely it will continue in the future. This is especially true in the electronic miniaturization and the increasing power output of electrical equipment. Efficient thermal management is imperative for these applications, since the improvement in the heat elimination of such devices is directly related to their improved efficiency, lengthening of half-life time operating and the prevention of premature failures or

1

damage of equipment. The electron circulation in materials produces heat by Joule effect and this heat must be removed from devices in order to maintain their work temperature. The electronic packing materials must disperse the heat produced to lower temperature, but also must possess low dielectric constant and low dielectric loss to avoid the signal distortion, which in turn provides better equipment performance.[1,2,3] It is know, that the reliability of an electronic device is exponentially related to the operating temperature of the junction. Therefore, a small difference in the operating temperature (10–15 °C) can result in a twofold reduction in the lifespan of the device.[4] Thus, thermal dissipation is a challenging problem and the development of new highly thermally conductive but electrically insulating materials is of capital interest to address this challenge.[5,6]

Epoxy resins have been recognized as versatile materials with good properties extensively used in the fields of electric and electronic industries as encapsulants, packaging or coatings, in printed circuit boards, integrated circuit chips and a huge range of electronic devices, electrical and communication equipment and lighting appliances.[7-10] Apart from brittleness, due to their high cross-linking density, one of the drawbacks of these materials is the very low thermal conductivity that exhibit (~0.2 W/m·K), which is mainly attributed to phonon scattering.[2,8,11,12] Some liquid crystalline epoxy thermosets, with ordered structure, can promote the movement of phonons, giving rise to thermal conductivity until 1 W/m·K, but the cost to fabricated them increase considerably.[3]

Much more convenient from the technological and economical point of view is the introduction of conductive fillers as an effective method to solve thermal conductivity drawbacks of epoxy resins.[11,13,14] Metallic particles or carbon materials, like carbon nanotubes (CNT), graphene and graphite, could be attractive fillers due to their high thermal conductivity, but they can make materials electrically conductive. Thus, they are useless to encapsulate electronic devices although they are important in aerospace and aeronautics technologies, where high-performance composites replace metallic materials in some applications to save weight.[4,15-17] Also metallic fillers have several disadvantages including high density and they are susceptible to oxidation.[18] For this reason, only selected fillers with high thermal conductivity and acceptable dielectric breakdown strength, such as some inorganic materials, can be used in order to maintain electrical insulation of composites.[3,19]

Among common inorganic particles, boron nitride (BN) provides the best combination of properties in terms of high thermal conductivity, low dielectric constant, high electrical resistivity and low coefficient of thermal expansion (CTE). Besides all this, BN also presents low density (2.2 g/cm$^3$),

2

high mechanical strength, high aspect ratio and chemical and thermal stability. BN can be synthesized in hexagonal and cubic forms. In particular hexagonal-BN, known as "white graphite", is a platelet-shaped synthetic ceramic, with a crystal structure similar to graphite (hexagonal layer crystals) except for the stacking of layers, its layered lattice structure give BN good lubricating properties.[6,11,13,20] The hexagonal BN layers are bonded by weak van der Waals forces, which enable the layers to slide easily against each other. These are the reasons for which BN has been selected in the present study to prepare new materials with enhanced thermal conductivity from epoxy matrices.

Most of the studies performed in epoxy BN composites are based in epoxy-amine or epoxy-anhydride matrices.[14] However, the curing by homopolymerization of epoxides carries several advantages and broadens the field of applications of this type of materials. Homopolymerization of epoxies can be done by cationic or anionic initiators, in both thermal and photoirradiation conditions.[21,22] Although the use of thermal latent cationic initiators for epoxy curing has not been much studied, it has superior advantages, especially in advanced processing technologies. Under environmental conditions the previously prepared formulations are stable and, only show activity by external stimulation on reaching high temperatures and once initiated they present high curing rates.[21,23-27] In this way, an effective control of initiation and curing process by heating leads to desirable advantages in handling and storage stability and makes these curing systems very advantageous in terms of energy saving and eco-friendly processing compared with conventional curing agents like polyfunctional amines or organic anhydrides. It should be emphasized that heating is easier than photoirradiation for practical use since homogeneous heating of reaction mixtures can be easily attained. Moreover, homogeneous photoirradiation has a higher difficulty since the irradiation area depends on the irradiation source. Thick samples are difficult to completely cure and shadowed areas remain unaltered. [28]

In the present work, an optimization of a latent cationic epoxy system to prepare BN composite materials with enhanced thermal conductivity has been carried out from the point of view of the kinetics. As the base resin, we used diglycidyl ether of Bisphenol A (DGEBA) and a commercially available quaternary ammonium-antimonium hexafluoride salt as initiator. This benzylanilinium salt was previously developed by Endo et al.[29] and has shown a good compatibility on adding several proportions of BN as filler. The kinetic studies of the curing have been performed by differential scanning calorimetry and the processability has been determined by rheological measurements. The BN-composites obtained have been characterized by thermogravimetric and thermomechanical analysis and mechanical

characteristics like adhesion, hardness and impact resistance have been evaluated and compared to the unfilled material. The thermal conductivity and other parameters like thermal expansion coefficient, dielectric breakdown strength or electric resistivity have also been determined.

## 2. Experimental

### 2.1. Materials

DGEBA from Huntsman International LLC., Araldite GY 240 (EEW=182 g/eq.) was dried at 80°C under vacuum for 6h before use. Initiator CXC1612, from King Industries Inc., USA, was solubilised in propylene carbonate at 50 wt %. Propylene carbonate, distilled before use, was provided by Sigma-Aldrich Co. Ltd. Glycerol, supplied by Sigma-Aldrich Co. Ltd., was used as received. BN was purchased by ESK Ceramics GmbH, TPC 006, with a particle size of ~6µm.

### 2.2. Sample preparation

All the samples were prepared by weight, by adding varying initiator and glycerol proportions from 1 to 4 and from 0 to 8 phr (parts per hundred of resin) respectively to the DGEBA resin. For composite samples, the required amount of BN was added in wt. % to the previous formulation. The samples were mechanically stirred until homogeneous mixture and degassed under vacuum to prevent the appearance of bubbles during curing process. Finally, the samples were poured onto aluminium moulds and cured at 120°C for 1h, followed by a post-curing at 150°C for another 1h.

### 2.3. Characterization techniques

A differential scanning calorimeter (DSC) Mettler DSC-821e calibrated using an indium standard (heat flow calibration) and an indium-lead-zinc standard (temperature calibration) was used to analyse epoxy system. Samples of approximately 5-10 mg were tested in aluminium pans with a pierced lid in a nitrogen atmosphere with a gas flow of 100 mL/min. The dynamic studies were performed in a temperature range of 30-250°C with a heating rate of 10 K/min. Enthalpy (Δh) of samples was calculated by integration of the calorimetric signal. The glass transition temperature ($T_g$) of cured samples was determined in a second scan as the temperature of the half-way point of the jump in the heat capacity when the material changed from glassy to the rubbery state under nitrogen atmosphere. The error is estimated to be approximately ±1°C.

The curing kinetics was analyzed by means of isoconversional integral and Coats-Redfern[30] procedures applied to non-isothermal DSC experiments at heating rates of 5, 10, 15 and 20 ºC/min. Details of the kinetic methodology are given in previous studies.[31]

The thermal stability of cured samples was studied by thermogravimetric analysis (TGA), using a Metler TGA/SDTA 851e thermobalance. Experiments were performed under inert atmosphere ($N_2$ at 100 mL/min.). Pieces of cured samples of 10-15 mg were degraded between 30 and 600°C at a heating rate of 10 K/min. Also experiments in oxidant atmosphere were performed (synthetic air at 100 mL/min) to measure stability of the composite and BN residues in the samples, at the same heating rate between 30 and 800°C.

Dynamic mechanical thermal analyses (DMTA) were carried out with a TA Instruments DMA Q800 analyzer. The samples were cured isothermally in an aluminium mould a 120°C for 1h and a post-curing of 150°C for another 1h. Prismatic rectangular samples (15 x 7.3 x 2.4 mm$^3$) were analyzed by 3-point bending at a heating rate of 3 K/min from 35 to 195°C, the temperature at which rubbery state was observed, using a frequency of 1 Hz and oscillation of 0.1% of sample deformation. The Young modulus (*E*) was determined at 35°C by means of a force ramp at a constant rate, 1 N/min, never exceeding 0.25% of deformation to make sure that only elasticity was evaluated, linear zone of stress-strain graph. The slope between 0.1% and 0.2% of deformation was taken. *E* was calculated using the slope of the load deflection curve in accordance with the following equation:

$$E = \frac{L^3 m}{4bt^3} \qquad (1)$$

where *E* is the elastic modulus of epoxy sample (MPa), *L* is the support span (mm), *b* and *t* are the width and the thickness of test sample (mm) and *m* is the gradient of the slope (N/mm).

Thermomechanical analyses (TMA) were carried out on a Mettler TMA40 thermomechanical analyzer. Cured samples (9 x 9 x 2.2 mm$^3$) were supported by the clamp and one silica disc to distribute uniformly the force and heated at 5°C/min from 35 up to 200°C by application of a force of 0.01N, a minimum force to not distort the results. Two heating were performed, the first one to erase the thermal history and the second one to determine the thermal expansion coefficients (CTEs), below and above the $T_g$, calculated as follows:

$$CTE = \frac{1}{L_0} \cdot \frac{dL}{dT} = \frac{1}{L_0} \cdot \frac{dL/dt}{dT/dt} \qquad (2)$$

where *L* is the thickness of sample, $L_0$ the initial length, *t* the time, *T* the temperature and *dT/dt* the heating rate.

5

Impact test was performed at room temperature by means of a Zwick 5110 impact tester according to ASTM D 4508-10 using rectangular samples (25x12x2.3 mm³), cured in the same way of the other techniques. The pendulum employed had a kinetic energy of 0.56 J. For each material a minimum of 7 determinations were made with a confidence level of 95%. The impact strength (*IS*) was calculated from the energy absorbed by the sample upon fracture as:

$$IS = \frac{E - E_0}{S} \qquad (3)$$

where $E$ and $E_0$ are the energy loss of the pendulum with and without sample respectively, and $S$ is the cross-section of the samples. The fracture area of impact samples was observed with ESEM (environmental scanning electron microscopy) Quanta 600.

Microindentation Knoop hardness was measured with a Wilson Wolpert 401 MAV device following ASTM D1474-13. For each material a minimum of 20 determinations were made with a confidence level of 95%. The Knoop microindentation hardness (KHN) was calculated from the following equation:

$$KHN = \frac{L}{A_P} = \frac{L}{l^2 C_P} \qquad (4)$$

where $L$ is the load applied to the indenter (0.025 Kg), $A_P$ is the projected area of indentation in mm², $C_P$ is the indenter constant (7.028 x 10⁻²) relating $l^2$ to $A_P$.

Rheometric measurements were carried out in parallel aluminium plates (geometry of 25 mm Ø) mode with a TA AR G2 rheometer, equipped with electrical heated plates (EHP). Viscosity ($\eta$) and complex viscosity ($\eta^*$) of the pre-cured mixtures were recorded as function of shear rate (s⁻¹) and angular frequency $\omega$ (rad/s), respectively. In the case of $\eta^*$ with a constant deformation in the range of linear viscoelasticity for each mixture, obtained from constant shear elastic modulus ($G'$) in a strain sweep experiment at 1 Hz, always at 35°C. The curing was monitored at 90°C in order to determine the gel point and the conversion at gelation. Gel time was taken as the point where tan δ is independent of frequency.[32] The conversion at the gelation ($x_{gel}$) was determined by stopping the rheology experiment at gelation taking a sample and quenched in liquid nitrogen, and performing a subsequent dynamic DSC scan at 10 K/min of the gelled sample. The degree of conversion in the gelation point was calculated as follows:

$$x_{gel} = 1 - \frac{\Delta h_g}{\Delta h_T} \qquad (5)$$

where $\Delta h_g$ is the heat released up of gelled samples, obtained by integration of the calorimetric signal, and $\Delta h_T$ is the heat associated with the complete conversion of all reactive groups.

Adhesion test of the different mixtures on rectangular steel plates were done by tensile lap-shear strength of bonded assemblies' method by Houndsfield H10KS universal test machine with a 10kN load cell, following ASTM D 1002-10. At least, eight samples were tested for each mixture. The plate measures were 100 mm x 25 mm in plane and 1.5 mm in thickness. The overlap regions, 12.5 mm (± 0.25 mm) x 25 mm, were gently abraded with emery paper (320 grade) in two directions in 45 degrees to optimize the adhesion of the plates. The resin was cured in the oven for 3h at 170°C, followed by a post curing of 3h at 200°C. The apparent lap-shear strength ($\tau$) was calculated following:

$$\tau = \frac{P}{A} \qquad (6)$$

where $P$ the maximum load until fracture and $A$ the overlapping area.

Thermal conductivities were measured by a Transient Hot Bridge THB 100 from Linseis Messgeräte GmbH. The sensor was a HTP G 9161 with a 3 x 3 $mm^2$ of area. Two equal polished rectangular samples (15x12x2.2 $mm^3$) were placed in each one of the faces of the sensor. Due to the small size of sensor, side effect can be neglected. A measuring time of 100 s with a current of 10 mA was applied to each of the five measures done for different formulation.

Dielectric breakdown strength was measured using a Lamsa TD-51 alternating current dielectric strength tester, with a voltage supplied of 6.6 kV, 50 Hz transformer, according to ASTM D 149-09. Tests were made at room temperature with point/plane electrodes. The rate of voltage rising speed was 1 kV/s until breakdown. A minimum of 16 values were recorded for each specimen, discarding which ones flash over occur. Taking into account tabulated dielectric strength of epoxy resins (19.7 kV/mm) and BN (37.4 kV/mm)[33] and maximum voltage of tester, films of about 100-150 μm were prepared, by curing the composition between two Norton FEP Fluoropolymer films. Thickness measurements were made by a micrometer with rounded tips with a precision of ± 0.001 mm. Different results were obtained for each specimen and the data obtained may be represented by statistical distribution. Two-parameter Weibull distribution are used to obtain failure prediction response and reliability of the materials because of its advantages such as high accuracy of results even with few determinations and a confinable method to estimate useful life of materials. Distribution is written as:[34]

$$P = 1 - exp\big[(-E/E_0)^{\beta}\big] \qquad (7)$$

where $P$ is the cumulative probability of electrical failure, $E$ is the experimental breakdown strength, $E_0$ is the scale parameter, the characteristic breakdown strength at a cumulative failure probability of 63.2%, which is frequently used to compare different samples, and $\beta$ is the shape parameter, inversely proportional to deviation of data. For failure probability, IEEE 930-2004 standard recommends a good, simple approximation:[35]

$$P_i = \frac{i-0.44}{n+0.25} \cdot 100\% \qquad (8)$$

where $i$ is the i-th result when values of E are sorted in ascending order, and $n$ the number of samples.

Volume resistivity of samples was measured on a Metrel MI 2077 TeraOhm 5 kV insulation tester at room temperature. Pieces of 2.2 x 12 x 17 mm$^3$ were essayed between stainless steel circular electrodes with an area of 19.655 mm$^2$ placed on both faces of samples. The applied voltage to the thermosetting composites were 5 kV for 1 min. Electrical resistivity ($\rho$) of uniform cross sectional materials can be determined by:

$$\rho = R\frac{A}{l} \qquad (9)$$

where $R$ is the resistance measured by the apparatus, $A$ and $l$ the area and the thickness of sample.

### 3. Results and discussion

3.1. Optimization of the curing process of the neat and BN modified formulations

Initiators are important in curing processes since they have a catalytic effect and decrease the activation energies, accelerating the process. In cationic systems, not only the cation plays a role, but also the anion can increase the reactivity of the system if it has a low nucleophilicity, minimizing or preventing the reaction of the cationic growing chain with the anionic species.

The cationic homopolymerization of epoxides initiated by benzylanilinium salts was firstly developed by Endo's group.[23,24,29] The catalyst N-(p-methoxybenzyl)-N,N-dimethylanilinium hexafluoroantimonate has been selected for the present study and is commercialized as CXC 1612. The structure of this compound was determined by NMR spectroscopy and the spectra and the thermal behaviour fit well with the data reported.[23,24] It was also demonstrated by the same authors, that on heating, benzyl cations are released, which are the true catalytic species that initiate the attack to the oxiranic oxygen. As anion, hexafluoroantimoniate compensate the positive charge and has a very low nucleophilicity, which is required to avoid termination of epoxy homopolymerization.

8

Cationic epoxide homopolymerization follows two different mechanisms, known as AM (activated monomer) and ACE (active chain end). Both mechanisms are depicted in **Scheme 1**. AM mechanism is favoured in the presence of OH groups.[36,37]
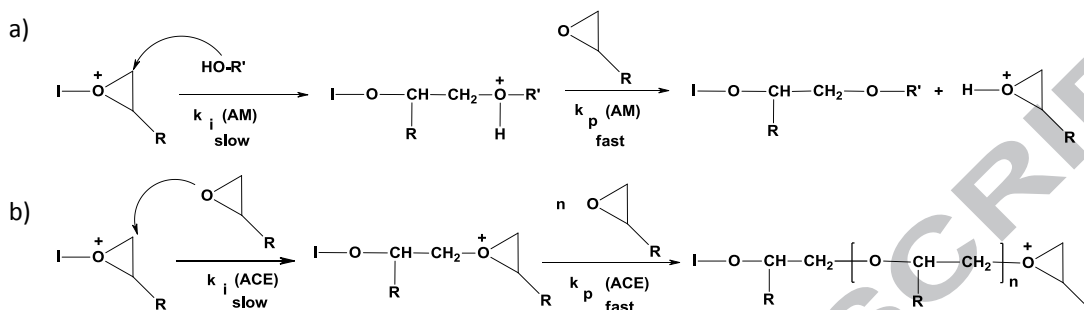


**Scheme 1.** Activated monomer mechanism (a) and active chain end mechanism (b).

Both processes compete and in some cases they were detected by calorimetric scans.[38,39] The proportion of hydroxyl groups can influence the global propagation rate. In addition to the initiation and chain growing, inter and intramolecular transfer processes can occur besides to termination reactions. This is due to the fact that this epoxide ring-opening mechanism follows a chain-wise polymerization pattern. Therefore, the kinetics of the cationic curing should be studied from the process as a whole. As the first step of the work, the optimization of the composition of the neat formulation (without BN) was performed be means of DSC studies (kinetics of curing) and other techniques like DMTA and TGA, to reach the most adequate characteristics of the final material. First, we studied the evolution of the curing process by varying the proportion of initiator (from 1 to 4 phr) by means of calorimetric studies. **Figure 1A** shows the DSC curves corresponding to this process.
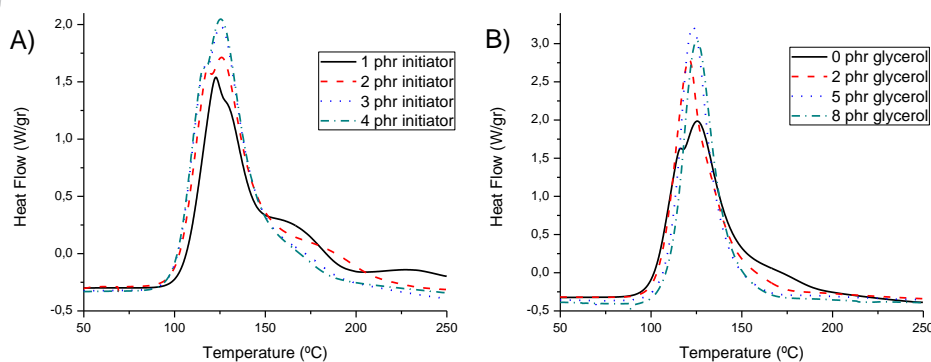


**Figure 1.** DSC curves showing the effect of the different proportions of initiator (A) and adding different proportions of glycerol (B) in the curing process.

We can see in the figure that the curing process starts at slightly lower temperatures with the increasing proportion of initiator, although the difference is scarce from 3 to 4 phr of catalyst. However, a little difference in the shape of the curves is noticeable on varying the proportion of initiator. The highest peak at lower temperature has a complex shape that can be attributed to the coexistence of AM and ACE mechanisms that occurs overlapped giving rise to a certain splitting in the exotherm. As the process AM is faster,[40] it is assumed that the first peak is due to this mechanism.[21,37,38] Also, a shoulder after the maximum can be observed, decreasing when the proportion of initiator increases. These shoulders are sometimes due to phenomenological issues like vitrification or to thermal epoxy homolymerization. **Table 1** shows the most important data extracted from the calorimetric analysis.

**Table 1**. Calorimetric data of formulations of DGEBA with several proportions of initiator and glycerol.

| Initiator (phr) | Glycerol (phr) | $T_{max}{}^a$ (°C) | $\Delta h^b$ (J/g) | $\Delta h^b$ (kJ/ee) | $T_g{}^c$ (°C) |
|---|---|---|---|---|---|
| 1 | 0 | 122 | 381 | 71 | 121 |
| 2 | 0 | 125 | 502 | 95 | 152 |
| 3 | 0 | 124 | 531 | 102 | 135 |
| 4 | 0 | 125 | 523 | 103 | 131 |
| 3 | 2 | 120 | 504 | 99 | 129 |
| 3 | 5 | 122 | 481 | 97 | 122 |
| 3 | 8 | 124 | 483 | 100 | 120 |

[a] Temperature of the maximum of the curing exotherm.
[b] Enthalpy of the curing process by gram of mixture or by epoxy equivalent.
[c] Glass transition temperature determined by DSC in a second scan after a dynamic curing.

One of the most important calorimetric parameters is the heat evolved during the curing process, which can be expressed by gram or by epoxy equivalent. If we look to the heat released by epoxy equivalent we can evaluate if the curing has been completed. It is reported that the enthalpy evolved by epoxy equivalent in a complete curing is about 100 kJ/ee,[41] and in principle, the maximum heat evolved the higher crosslinking degree reached. From the values of the table we can go to the conclusion that 3 phr of initiator is the best proportion to reach the curing with a quite good $T_g$ value and a simple shape of the curve without any shoulder at high temperature that usually leads to increase unnecessarily the curing time or temperature.

As we have introduced above, AM mechanism is favoured by the presence of hydroxyl groups and this mechanism is faster than ACE.[38] In order to facilitate the curing, we added small proportions of glycerol, which is a trifunctional alcohol that does not produce any reduction of the crosslinking density, as occurs in compounds with an only hydroxyl group.

As we can see in **Figure 1B**, the addition of a little amount of glycerol leads to a simplification of the curve, which turns unimodal. It is also noticeable than the temperature of the maximum of the peak is

maintained but the curing rate is increased according to a higher contribution of the AM mechanism on adding hydroxyl groups.[42] Also, the shoulder at higher temperature tends to disappear. Table 1 shows the most significant data extracted from DSC curves.

The addition of glycerol to the reactive mixture does not affect negatively the evolution of the curing or the enthalpy released but it can influence the network structure and therefore thermomechanical and thermostability should be evaluated. By looking to the values in the table, we can see that there is a difference in the glass transition temperature reached in the cured material. The higher the proportion of glycerol in the formulation the lower the Tg. This can be explained by the contribution of two different factors: the flexible structure of the glycerol and that AM mechanism, which leads to chain transfer processes, which limits the growing of the chain, reducing the crosslinking degree. The stability to high temperature of these materials was evaluated by thermogravimetry. **Table 2** collects the most representative data extracted by TGA.

**Table 2**. Thermogravimetric and thermomechanical data on varying the glycerol proportion in DGEBA formulations with 3 phr of initiator.

| Glycerol (phr) | $T_{2\%}$ [a] (°C) | $T_{max}$ [b] (°C) | Char yield[c] (%) | Young modulus[d] (GPa) | $T_{tan \delta}$ [e] (°C) | E'[f] (MPa) |
|---|---|---|---|---|---|---|
| 0 | 306 | 432 | 14.1 | 2.0 | 147 | 50 |
| 2 | 310 | 433 | 13.4 | 2.3 | 138 | 44 |
| 5 | 300 | 432 | 11.2 | 2.4 | 122 | 25 |
| 8 | 154 | 432 | 9.2 | _[g] | _[g] | _[g] |

[a] Temperature of decomposition in TGA calculated for a 2% of weight loss.
[b] Temperature of the maximum decomposition rate determined by TGA in $N_2$ at 10°C/min.
[c] Char residue at 600°C.
[d] Young modulus determined by DMTA at 35°C by the three point bending mode
[e] Temperature of maximum of the tan δ at 1 Hz.
[f] Relaxed modulus determined at the $T_{tan \delta}$ + 40°C (in the rubber state).
[g] Not determined

As can be seen in the table, the sample with 8 phr of glycerol presents an initial weight loss at low temperature and a lower char yield that could be attributed to the fact that not all the glycerol molecules have been chemically incorporated to the network. In fact, exudation phenomena was observed in samples containing 8 phr of glycerol during storage, which confirms that some proportion of glycerol remained unreacted in the cured material. According to that, this formulation has not been further tested.

Then, DMTA analyses were carried out. The increase of glycerol proportion provides an enhancement of Young modulus. The increase is higher on adding little proportions of glycerol (2 phr) and then a minor effect is observed on adding 5 phr. However, temperature of the α relaxation and modulus in the rubbery state decrease, especially when 5 phr of glycerol was in the formulation. By

11

taking into consideration all these data and the reactivity observed by DSC we selected as the most adequate formulation for the base material, the one constituted by 3 phr of cationic initiator and 2 phr of glycerol as additive of DGEBA resin that meets the best compromise. It should be commented that this formulation keeps its latent characteristics, since the storage at room temperature for three months leads only to a slight decrease of a 1% in the heat evolved during curing.

Once selected the base epoxy formulation, different proportions of BN were added with the aim to enhance thermoconductivity and the effect in several characteristics in the final thermosets. The proportion of BN in these DGEBA formulations is limited to the 20% in weight, since higher amounts of this filler rends too high viscosity to the formulation and big difficulties to reach homogeneous mixtures, without use of solvents. The different formulations prepared were analysed by calorimetry to investigate their reactivity on curing and the calorimetric curves are represented in **Figure 2**.
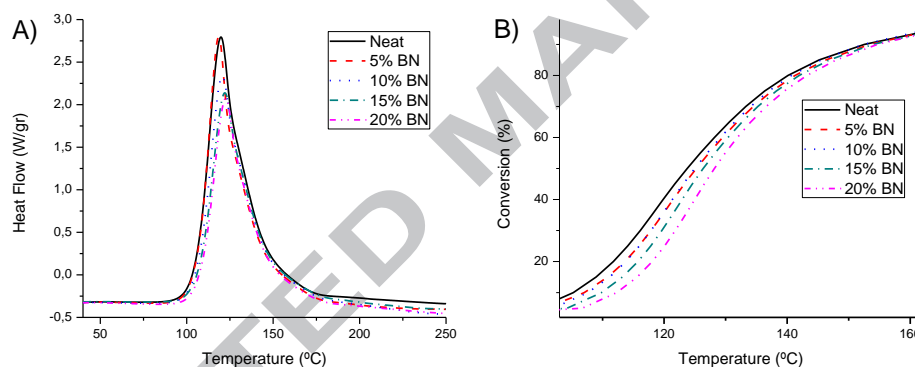


**Figure 2.** (A) DSC curves showing the effect of the addition of different proportions of BN to the neat formulation and (B) plot of conversion against temperature at 10 °C/min.

In the figure we can observe a slight shift of the exotherms at higher temperatures on increasing the proportion of filler in the formulation and also a decrease in the height of these curves, both indicating a reduction in the reactivity. The fact that the shape of the curves is similar and all formulations begin the curing at the same temperature confirms that the latency is kept unaltered. It is worth noting, that in the plots of conversion against temperature the bigger differences in reactivity appear at low temperatures and are proportional to the amount of BN in the formulation. From these results, it can be stated that BN does not participate in the homopolymerization mechanism due to its inert character and does not affect the active cationic species. However, the reduction expected by the dilution of epoxide groups or the hindrance produced by the BN particles have been detected. It should be noted that in BN sheets, the basal plane is molecularly smooth and has no surface functional groups available for chemical bonding or interaction. Only the edge planes of the BN platelets do have functional groups such as hydroxyl groups

12

(-OH) and amino groups (-NH$_2$).[43] OH groups, although scarce, could participate in the AM mechanism producing not only a little effect on the kinetics, but also helping to form some covalent bonds between the BN particles and the epoxy matrix.[44] Amino groups can also help to increase the BN-epoxy interactions. The most representative data extracted from the calorimetric study are collected in **Table 3**.

**Table 3.** Calorimetric data on varying the BN proportion in DGEBA formulation with 3 phr of initiator and 2 phr of glycerol

| % BN | $T_{max}$[a] (°C) | $\Delta h$[b] (J/g) | $\Delta h$[b] (kJ/ee) | $T_g$[c] (°C) | $E_a$[d] (kJ/mol) | ln A[e] (min$^{-1}$) | $k_{120°}$[f] (min$^{-1}$) |
|---|---|---|---|---|---|---|---|
| 0 | 120 | 504 | 99 | 129 | 127.1 | 38.4 | 0.65 |
| 5 | 119 | 469 | 97 | 129 | 144.0 | 43.6 | 0.61 |
| 10 | 121 | 459 | 100 | 129 | 135.7 | 40.9 | 0.56 |
| 15 | 122 | 420 | 97 | 130 | 122.3 | 36.7 | 0.47 |
| 20 | 123 | 394 | 97 | 130 | 121.1 | 36.2 | 0.42 |

[a] Temperature of the maximum of the curing exotherm.

[b] Enthalpy of the curing process by gram of mixture or by epoxy equivalent.

[c] Glass transition temperature determined by DSC in a second scan after a dynamic curing.

[d] Activation energy at 0.5 of conversion evaluated by isoconversional non-isothermal integral procedure KAS.

[e] Values of pre-exponential factor at 0.5 of conversion for second order (*n*=2) kinetic model with g(α)=-1+(1-α)$^{-1}$.

[f] Rate constant at 0.5 of conversion determined by using Arrhenius equation.

The data do not show any significant difference in the heat evolved by epoxy equivalent, which indicates that the curing is completed even in formulations with high proportions of BN. However, the heat evolved by gram of mixture is decreasing, because of the lower proportions of epoxide on increasing the filler percentage. The differences in the T$_g$ are not relevant, which seems to support that the type of network formed remains unaltered and that the balance between AM and ACE mechanism does not change by the addition of BN to the formulation.

By KAS isoconversional kinetic analysis, it was observed that the activation energy barely changes with the conversion (results do not show). This result confirms that the kinetic reaction mechanism is constant during curing and suggests that the kinetic model can be determined by Coats Redfern procedure. Using this methodology it was determined that all formulations follow a second order kinetic model with *n* = 2, as it is expected for cationic epoxy homopolymerization. Table 3 shows, as an example, the kinetic parameters for all formulations at conversion of 0.5. Activation energies and pre-exponential factor varies in a non-regular trend on increasing the proportion of BN in the formulation. In many reaction processes the variations in activation energy do not actually reflect kinetic changes, due to the compensation effect between the activation energy and the pre-exponential factor.[45] The value of the rate constant is a better reflection of the actual kinetic changes, since it includes both the effect of the

activation energy and the pre-exponential factor. It can be observed as the rate constant is reduced on increasing BN content (Table 3), according to the retarding effect exerted of BN and in agreement with the calorimetric data (Fig. 2B). This behaviour can be attributed to the increased viscosity of the formulation and to the dilution effect of BN.

3.2. Rheological study of the BN formulations

Rheological analysis can provide insights into the evolution of the structure of BN networks, interactions between BN and polymer chains, and the dispersion of BN sheets in the matrix. This type of mixtures have complex rheological properties and depend on many factors such as particle size, particle shape, volume fraction of filler and the applied shear rate. In the same way the interactions particle-particle and particle-matrix play an important role.[46,47] Accurate measurements of viscosity are absolutely necessary for understanding these interactions, control and optimize process conditions and product performance and computer simulations.[48] Thus, the formulations with different amounts of BN were investigated by this technique.

The first point to consider is the Newtonian behaviour of the unfilled resin (**Figure 3**). The experimental data exhibited some usual properties of suspensions of particles in Newtonian fluids: unbounded viscosities at low shear rates (yield stress), strain dependent properties and shear thinning.[47] These effects are the results of the changes in the structure generated by particle interactions causing redistribution of particles and their orientations. The flow study showed that with the increasing of BN particles, as found by Han and Lem with different fillers,[49] the viscosity is raised more than two orders of magnitude and the degree of shear thinning at low shear rates was highly increased, as it is shown in **Figure 3**.
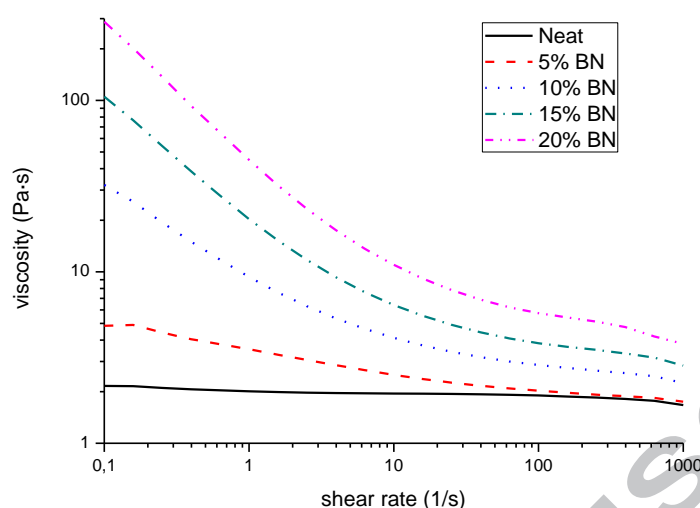
**Figure 3.** Plot of log η *versus* log ν for the different formulations at 35°C from 0.1 to 1000 s$^{-1}$.

This effect is accompanied with a Newtonian asymptote at high shear rates. This observation is in accordance with previous results in the field of layered silicate-polymer systems.[50] This rheological behaviour is determined by the balance of hydrodynamic force, that tend to align the major axis with the flow, and rotary Brownian motion (non-hydrodynamic forces) that tends to randomize the orientation. Brownian motion are negligible for the shape, distance between particles and dimensions (>1μm) of BN particles in more concentrated blends (yield stress and shear thinning),[51] which explain the diminution of η when the shear rate is increased. In the neat solution (Newtonian behaviour) and 5 wt. % of BN concentration (pseudoplastic) Brownian diffusion predominates and then the dispersion may be considered dilute.

Oscillatory experiments were performed to determine the viscoelastic response of material. It is known that complex viscosity (η*) and the dynamic storage modulus (*G'*) are extremely sensitive to the microstructure variation of filler reinforced polymer mixtures. The Newtonian behaviour is practically kept constant in all the range of strain studied for the base formulation. However, this range becomes shorter and goes to lower strains on increasing the filler content in the strain sweep experiments, where the frequency is fixed (1 Hz) (see **Figure 4A**). The linear viscoelastic region, where the G' are independent of the applied strain, found a critical strain above which the structure starts to breakdown earlier when the amount of filler is raising.[52] Then, the strain was fixed in the linear region for each mixture to perform the oscillatory sweep tests, measuring parameters as function of frequency. As in η plot, η* showed analogous behaviour finding significant change between composites with BN

15

concentration below 5 wt. % and above, nearly Newtonian plateau and shear thinning, respectively, in all the frequency range tested (**Figure 4B**), but more pronounced at low frequencies.
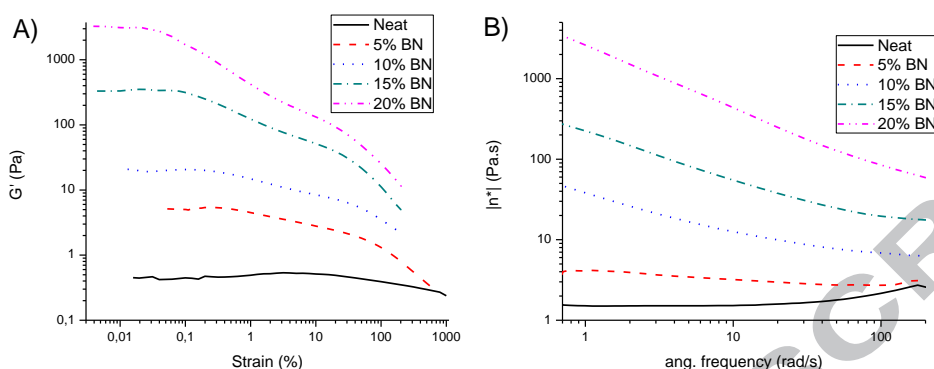


**Figure 4.** (A) Plot of log G' *versus* log % strain in oscillatory experiments (1 Hz). (B) Plot of log η* *versus* log ω, both at 35°C for all the formulations.

This behaviour is due to the increase in G' and loss modulus (G'') and can be ascribed to the alignment of the particles and their interactions when a stress is applied. It is interesting to note the small increase in viscosity of the unfilled and low filled compositions when frequency exceeded certain critical value. This apparent increase is associated with the entrance of turbulent regime, but does not mean that viscosity increases, indicates that the degree of turbulence grows.[51] G' (elastic property) and loss G'' (viscous property) curves as a function of frequency of all the formulations are represented in **Figure 5**.
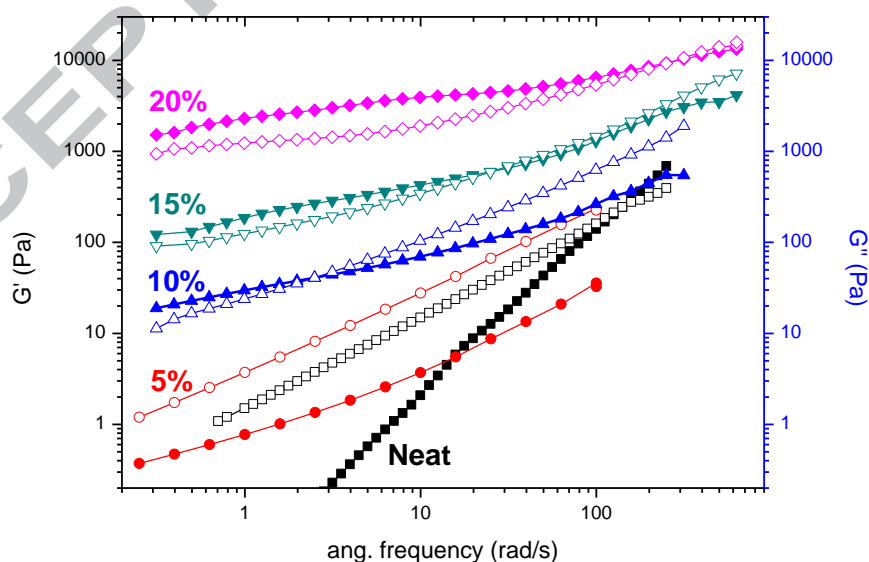


**Figure 5.** Plots of G' (filled symbols) and G'' (open symbols) against ω of formulations at 35°C.

How is expected, unfilled resin greatly follows the linear rheological theory (G' $\propto \omega^2$ and G'' $\propto \omega^1$) at low frequency. Nevertheless, the slopes decrease monotonically with increasing BN content. When

16

the concentration exceeds 5 wt. % there is a sharp falling in the slope at low angular frequency, indicating a significant variation of the microstructure of composites. G' is observed to be almost independent of the frequency when the filler loading is above that concentration. Also, the change in the liquid like behavior (G' < G'') to solid like (G' > G'') is observed. This change in G' at about 10 wt. %, with a kind of plateau at low frequency, means that composites have reached a rheological percolation. Near the percolation threshold, theory predicts a power law relation that can be used (adapting to mass fraction instead of volume fraction)[53,54] at fixed frequency to determine the threshold of the rheological percolation.[55,56]

$$G' \propto (m - m_c)^{\beta} \quad (10)$$

where $G'$ is the storage modulus, $m$ is the mass fraction of BN composites, $m_c$ is the mass fraction at rheological percolation and $\beta$ is the critical exponent. This relation is often valid only on a very narrow concentration region.[48] The rheological percolation at 1 rad/s and 10 rad/s was calculated to be 6.9 wt. % and the critical exponent 1.9.

Gelation is an irreversible phenomenon taking place during curing and processing of epoxy formulations that corresponds to the point at which the initial network is formed. Then, the gel fraction extends and increases crosslinking as the curing advances leading to an insoluble and three-dimensional network at the end of the curing process. Macroscopically, there is an abrupt change from a liquid-like to a solid-like behaviour and the viscosity tends to infinite. The material ceases to flow and starts to build up mechanical properties.[32] The knowledge of the conversion and gelation time is of capital importance from the industrial processing point of view that takes into account temperature, time and the minimum viscosity for injection or transfer moulding for computer chip packaging systems. Whereas, the prediction of the conversion at the gelation in polycondensation processes is quite easy by applying the Flory equation,[57] in chain-wise polymerization the conversion at the gelation depends in a complex way on the relative rate of initiation, propagation and termination and also on the amount of initiator. Increasing the initiator concentration results in shorter primary chains and a corresponding increase in the gel conversion, similarly occurs when increasing amounts of hydroxylic compounds are added to the formulation.[21] Since, ring-opening polymerization results from an initiation step starting at different times and positions in the curing mixture, the process is not as homogenous as in polycondensation mechanisms and inhomogeneities, called microgels, appear in the reactive mixture, leading sometimes to gelation at lower conversion than expected.[58]

17

The addition of BN to the formulation can influence both gel time and conversion at the gelation and the values obtained experimentally are collected in **Table 4**.

**Table 4.** Gelation data from rheometric monitoring of the curing of the formulations at 90°C.

| % BN | $t_{gel}$[a] (min) | $X_{gel}$[b] (%) |
|------|------------------|-----------------|
| 0 | 11.0 | 34 |
| 5 | 10.0 | 30 |
| 10 | 10.0 | 30 |
| 15 | 9.5 | 25 |
| 20 | 8.0 | 23 |

[a] Gel time determined from the frequency independent crossover of tan δ.
[b] Determined as the conversion reached by rheometry and DSC test at 10°C/min.

From the results obtained, it can be observed that there is a tendency to the reduction of the gel time on increasing BN concentration. The same behaviour was established by several authors when examined an epoxy resin system with silica filler.[59,60] Moreover, the conversion at the gelation diminishes on increasing the proportion of BN in the formulation. The decrease in the gelation time with increased filler concentration can be related to the fact that the conversion at gelation has decreased by the effect of the BN particles. This decrease could be related to the reaction of -OH and $-NH_2$ groups at the edge of the BN platelets, which can reduce the primary chain length.

3.3. Thermal characterization of the BN-composites

The addition of inorganic fillers, like BN, can modify the thermal behaviour of the polymeric matrix. Therefore, the thermal stability and the thermomechanical characteristics of the new BN composites were evaluated by TGA and DMTA. The most characteristic data obtained by TGA are collected in **Table 5**.

**Table 5.** Thermogravimetric data for the thermosets prepared by varying the concentration of BN

| % BN | $T_{5\%}$[a] (°C) | $T_{max}$[a] (°C) | Char Yield[b] (%) | $T_{5\%}$[c] (°C) | $T_{max}$[c] (°C) | Char Yield[d] (%) |
|------|------------------|-------------------|-------------------|-------------------|-------------------|-------------------|
| 0 | 390 | 433 | 13.4 | 343 | 429 | 0.0 |
| 5 | 393 | 434 | 18.1 | 368 | 429 | 4.9 |
| 10 | 392 | 433 | 23.1 | 369 | 428 | 10.4 |
| 15 | 394 | 433 | 28.1 | 373 | 429 | 15.1 |
| 20 | 393 | 432 | 32.6 | 379 | 430 | 20.0 |

[a] Temperatures of 5% weight loss and maximum decomposition rate determined by TGA in $N_2$ at 10°C/min.
[b] Char residue at 600°C (in $N_2$).
[c] Temperatures of 5% weight loss and the maximum decomposition rate determined by TGA in air at 10°C/min.
[d] Char residue at 800°C (in air).

From the TGA curves it can be confirmed that composites show similar degradation pattern that the neat epoxy matrix, indicating that the addition of BN does not much affect the degradation

mechanism. From the data in the table, it can be seen that the initial degradation temperature is not affected in inert atmosphere by the addition of BN, but increases slightly in air. Temperature of maximum degradation rate is not affected by BN and the biggest difference is shown in the residues after heating at high temperature in inert or oxidizing atmosphere, as expected. The char residue at 800°C in air atmosphere agrees with the percentage of BN in the material. The char yield in nitrogen atmosphere is higher on increasing the BN % due to the formation of carbonaceous residues on the BN filler particles. It is reported a slight increase in thermal stability on increasing the proportion of filler in epoxy-BN composites,[14] but this behaviour was not observed in the composites prepared.

By thermomechanical tests the effect of the presence of BN in the cured materials was observed. Although it was not the aim of the present study, by increasing the BN proportion in the material a notable enhancement of thermomechanical behaviour was proved. **Table 6** collects the values obtained by DTMA of all the composites and the neat material for comparison purposes. **Figure 6** represents the variation of storage modulus and tan δ against temperature for all these materials.

**Table 6**. Thermomechanical data of composites prepared varying BN concentration.

| % BN | Young's Modulus[a] (GPa) | T tan $\delta$[b] (°C) | E'[c] (MPa) | CTE$_{glass}$[d] ($10^{-6} \cdot K^{-1}$) | CTE$_{rubber}$[e] ($10^{-6} \cdot K^{-1}$) |
|------|------|------|------|------|------|
| 0 | 2.3 | 138 | 44 | 75 | 183 |
| 5 | 2.6 | 144 | 79 | 73 | 175 |
| 10 | 2.8 | 144 | 95 | 69 | 180 |
| 15 | 3.2 | 145 | 115 | 66 | 179 |
| 20 | 3.5 | 145 | 148 | 58 | 177 |

[a] Young's modulus determined with DMTA at 35°C in a controlled force experiment using a three point bending clamp.
[b] Temperature of maximum of the tan $\delta$ at 1 Hz.
[c] Relaxed modulus determined at the $T_{tan \delta}$ + 40°C (in the rubbery state).
[d] Thermal expansion coefficient of glassy state determined between 50-75°C.
[e] Thermal expansion coefficient in the rubber state determined between 170-190°C.
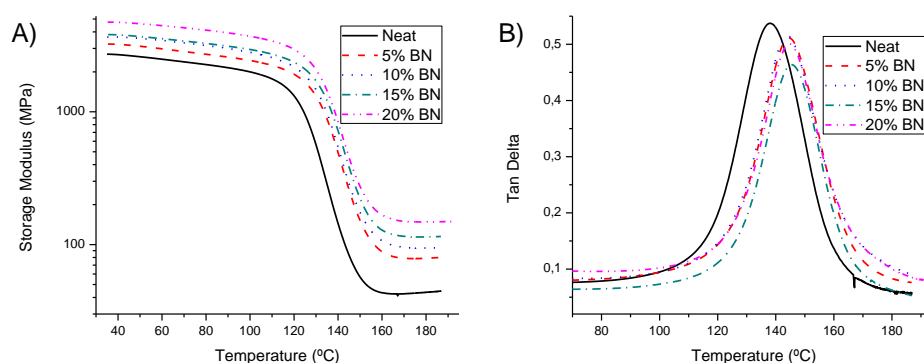


**Figure 6.** Variation of A) storage modulus and B) tan $\delta$ against temperature of the different materials prepared.

As we can see in the table, Young's modulus increases steadily on increasing the % of BN, which is more than a 50% in the sample with 20 wt. % of BN. It is also noticeable that the storage modulus in the rubbery state goes from 44 to 148 MPa, which is a consequence of the reinforcement produced by the filler. Unlike calorimetric study, by DTMA it was observed that on adding BN to the formulation, the composites showed an increase in the $T_g$ of 6-7 °C, although the final $T_g$ was independent from the thermoset composition. The different evolution of the $T_g$ value by DSC and DMTA can be attributed to the physical basis of both measurements. By calorimetry, only changes in the calorific capacity of the polymeric matrix can be detected while in DMTA, the mechanical effects of the filler in the relaxation phenomena of the polymer matrix can affect $T_g$ values. In a previous study on DGEBA/BN composites,[14] $T_g$ determined by DMTA was increased in 4-5 °C. The authors attributed this enhancement in the relaxation temperature to the surface functionalization of BN particles made by sol-gel with a reactive amine that increases the interaction filler-matrix. However, similar enhancements were obtained in the present work without any surface modification. Thus, from our results, we can state that a restriction of the chain motions for the presence of BN particles and a certain reaction of groups at the edge of the platelets together with some interface affinity between BN surface and epoxy matrix are the responsible for the improvement of temperature of the α relaxation.

Figure 6A shows in the DMTA curves an steadily increase on storage modulus on increasing the % BN in the material, which affects the vitreous and rubbery state, and a unimodal shape of tan δ curve, which indicates that a homogeneous material is formed even in case of high BN percentages.

Dimensional stability is an important consideration for epoxy materials used in many demanding areas, especially for electrical and electronic applications. Table 6 shows the CTE of the thermosets with different BN contents in the range below and above $T_g$ measured by TMA. As expected, the introduction of the ceramic filler produces a decrease in the CTE. The difference is more remarkable in the vitreous state, which will be the work temperature. This suggests that the mechanical interlock at the organic-inorganic interface may constrain the CTE mismatch of the components.[61] This behaviour, as with the $E$ modulus, will be beneficial in the use of these materials as adhesives or encapsulants in printed circuit boards. The more similar will be the properties of composite and metallic substrate, the minimum internal stress and crack will be produced by the temperature fluctuation, ensuring reliability of electronic devices when they run.

3.4. Mechanical characterization and dielectric properties of BN-composites

20

One of the most important shortcomings of epoxy thermosets is their fragile characteristics, due to the high crosslinking density and therefore, some toughness agents are added to the formulation to improve impact resistance. However, most of these agents decrease the $T_g$ and other thermomechanical properties, reducing the materials performance. In the present work, the addition of a little proportion of glycerol aims to introduce some more flexibility to the network structure and the addition of BN as the filler can also improve toughness by changing the fracture mechanism, especially if some interactions between particles and matrix exist. Toughness characteristics were evaluated by impact test. **Table 7** shows the values of impact strength for all the materials prepared. It can be seen, that the addition of BN leads to an improvement of the neat material in about a 75%, which is quite high. However, on increasing the proportion of BN in the material the increase produced is only slight.

**Table 7**. Mechanical and dielectric properties of the composites

| % BN | Impact strength (kJ/m$^2$) | KHN[a] | $\tau$[b] (MPa) | $E_0$[c] (kV/mm) | $\beta$ (shape parameter) | Resistivity ($\Omega \cdot m \cdot 10^9$) |
|---|---|---|---|---|---|---|
| 0 | 1.45 ± 0.15 | 21.91 ± 0.44 | 15.88 ± 1.51 | 30.8 | 7.2 | 5.4 |
| 5 | 2.31 ± 0.25 | 23.53 ± 0.63 | 14.99 ± 0.96 | 35.6 | 5.8 | 5.6 |
| 10 | 2.41 ± 0.10 | 27.93 ± 1.37 | 15.86 ± 0.56 | 38.7 | 6.5 | 5.8 |
| 15 | 2.51 ± 0.27 | 25.73 ± 0.87 | 14.90 ± 0.81 | 41.9 | 5.7 | 6.0 |
| 20 | 2.54 ± 0.25 | 25.19 ± 0.89 | 12.83 ± 0.86 | 42.8 | 8.7 | 7.6 |

[a] Knoop microindentation hardness.
[b] Apparent lap-shear strength.
[c] Scale parameter of Weibull distribution, the dielectric breakdown strength.

The fracture surfaces were examined by ESEM microscopy and **Figure 7** shows their appearance.
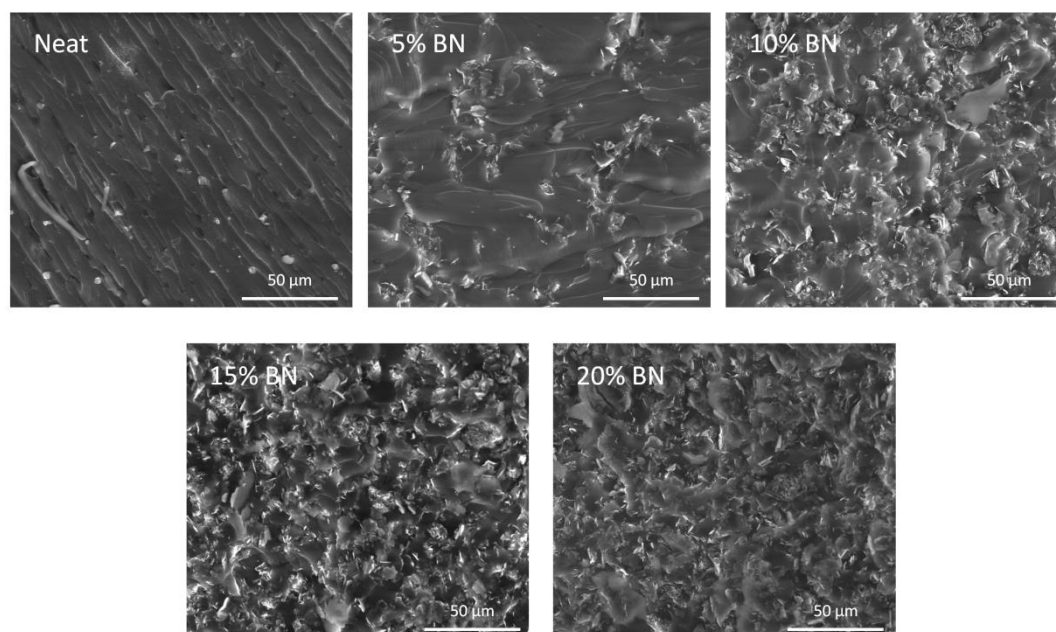
**Figure 7.** ESEM micrographs for the fracture surfaces of the materials prepared on varying the BN content at 800 magnifications.

It is worth to note the great difference between the micrograph of the neat and of the filled materials. When increasing the filler proportion, the roads of breakage appear shorter and less straight, which explains the increase in the impact strength by having to start new paths of brakeage. Likewise, it can be observed the homogeneity of the materials. There is also a great difference between the samples with 5 and 10% of BN. Whereas in the case of 5% sample, the BN particles are completely isolated and surrounded by the polymeric matrix, in the sample with 10% the particles are close to each other because of the percolation produced at filler contents in between (6.9%).

Microindentation hardness measurements rate the resistance of the material against penetration by static load. This parameter is of interest in the coatings industry. The results obtained using a Knoop microindenter are collected in table 7. As it can be seen, there is a slight tendency to increase hardness on increasing the proportion of BN in the material but it does not follow a linear increase but reach a maximum at 10% of filler added. In any case, BN does not worst but even improve this characteristic.

Adhesion is a complex property that depends on different factors, which include properties of the coating (viscosity, surface energy, etc.), substrate properties (roughness, surface energy, etc.), interfacial properties (internal stress, wettability, etc.) and environmental conditions (humidity, temperature, etc.). Also, differences in thermal expansion coefficients between substrate and coating lead to the reduction of adhesion, especially for epoxy coatings cured at high temperature, since the final decrease of temperature after curing creates internal stresses that leads to the production of microcracks, warping, etc. Internal stress generated during cooling increases proportionally to the differences between $T_g$ and curing temperature.[62] Table 7 shows the apparent shear strength values on steel surfaces for the different materials prepared with different BN content. As we can see, the neat material presents a good adhesion to the metal. This value, in general, does not experiment great changes on adding BN to the formulation, but the addition of a 20% of BN leads to a reduction in a 20% of this value. Taking into account that CTE decreases on increasing BN content (see Table 6), the slight reduction of lap-shear strength observed in table 7 could be related with the lower adhesion of BN particles to the metal than epoxy matrix.

Dielectric breakdown strength measurements were performed to determine the highest voltage which samples can stand before they fail electrically, divided by sample thickness. Weibull plots are presented in **Figure 8**. The addition of BN presented a clear trend to enhance electrical breakdown strength ($E_0$), also presented in table 7, in increasing the order of filled composites (5 to 20 wt. %).

Relative small shape parameters are attributed to imperfections such as imperceptible bubbles, microcracks or tiny fissures created during curing of the thin films.

Despite the fact that the introduction of defects can reduce the electric resistance, the addition of BN particles show a favorable behavior on growing their proportion. The increasing trend observed is according to previous published results.[13,63]
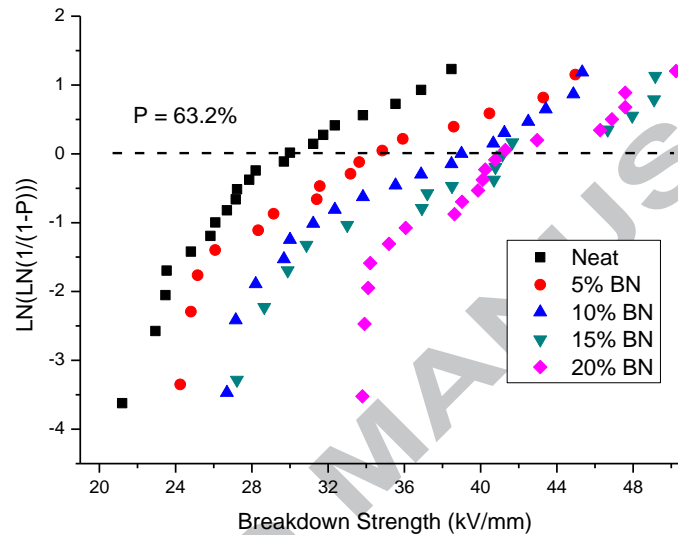


**Figure 8**. Weibull plots of breakdown strength for neat epoxy and the composites.

The same pattern was observed in the electrical resistivity of the composites (see table 7). This is the intrinsic property of materials that quantify the opposition to the current flow, another important property in the thermal management in electronic packaging giving them security and stability to the electronic components. Voltage of 5 kV was applied to obtain the best determinations according to the capacity of the tester. As can be seen in the table the resistivity increases with the amount of BN in the material, although slightly. However, when the material contained a 20% of BN this parameter increases notably, reaching an increase of 40% in reference to the neat material. Both dielectric strength and electrical resistivity confirm the tendency that increasing the amount of BN particles, dielectric properties improve, because of the intrinsic properties of boron nitride.

3.5. Thermal conductivity

**Figure 9** shows the variation of thermal conductivity with the filler content for BN resins. In general, the thermal conductivities of BN filled epoxy resins are enhanced with the increase of filler content. Although, h-BN has a high thermal conductivity (390 W/m·K in basal plane direction; and 2

W/m·K in the c-axis),[64] only limited amount of it is shared by the composite due to the presence of epoxy (k=0.2 W/m·K) used as the matrix. The thermal conductivity of the composites prepared in the present work improved linearly with the concentration of BN added getting a maximum of 0.61 W/m·K with the maximum concentration, 20% wt. (13.4 % in volume fraction). This constitutes an enhancement of more than 300% in reference to the neat epoxy.
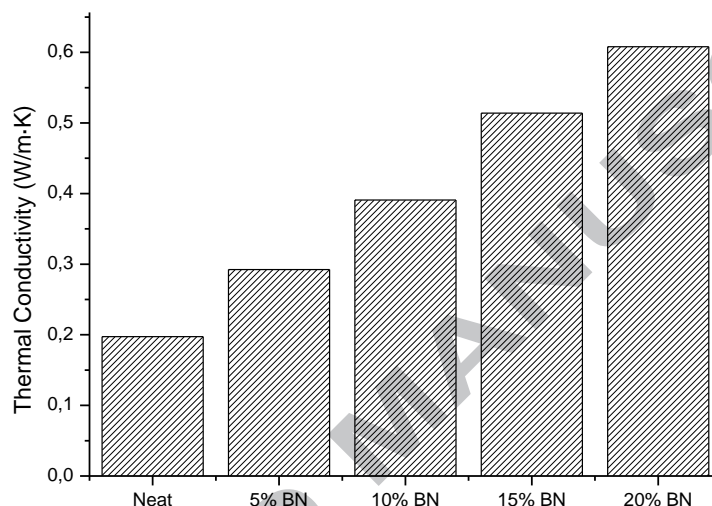


**Figure 9**. Thermal conductivity of the materials prepared on varying the BN content.

The thermal conductivity achieved an increase of 300% with the only addition of 20 wt% of BN to the formulation. If we compare the maximum conductivity achieved (with 13.4% of BN in volume) with other authors[14,63] we find equal or even better thermal transport characteristics. These authors stated that there was a great increasing when the addition of filler exceeded 20% in volume, which could not be accomplished in the present case because of the loss of homogeneity in the preparation of the mixtures, due to the high viscosity of the formulation. Taking into account the improvement of thermal conductivity along with other thermal, mechanical and electrical characteristics, it can be confirmed that the compounds prepared in this study are excellent materials for thermal dissipation applications.

### 4. Conclusions

A new latent cationic curing system for diglycidylether of bisphenol A was optimized. The curing behavior was not highly influenced by the addition of BN particles and it keeps the latency for a period of three months. The viscosity of the formulation raised with the addition of BN, which can explain, along with the dilution effect exerted by BN, the curing retardation experimented at lower temperatures.

24

Rheological studies allowed to determine that the Newtonian range became shorter and went to lower strains on increasing the filler content. The rheological percolation was calculated to be 6.9 wt. %.

On increasing the amount of BN in the formulation both the conversion at the gelation and the gelation time are reduced which seems to be related to the presence of OH and $NH_2$ groups in the BN structures which can reduce the primary chain length.

Glass transition temperatures, determined by DSC, were unaltered on increasing the BN proportion in the material, but slightly increased the tan δ temperature, because of the mechanical effect of the particles on relaxation phenomena. Young modulus and rubbery modulus increased steadily on increasing the % of BN.

The introduction of the ceramic filler produced a decrease in the thermal expansion coefficient, more remarkable in the vitreous state.

Mechanical characteristics were maintained or even improved. The addition of BN led to an enhancement in impact strength up to 75% in reference to the neat material. This effect was also confirmed by the SEM inspection of the fracture surface. Microindentation hardness reach a maximum at 10% of filler added in reference to the neat thermoset. Adhesion did not experiment great changes on adding BN to the formulation, but the addition of a 20% of BN led to a reduction in a 20% of this value.

Thermal conductivity enhancements of more than 300% in reference to the neat epoxy was reached, which increased proportionally to the % BN content. Both dielectric strength and electrical resistivity confirm the tendency that increasing the amount of BN particles, dielectric properties improved, because of the intrinsic properties of boron nitride added to the formulation.

## 5.  Acknowledgments

## 6.  References

[1] Thermal Conductivity: Theory, Properties, and Applications. Tritt TM, editor. Springer US, Kluver Academic/Plenum Press, New York, 2004.

[2] Burger N, Laachachi A, Ferriol M, Lutz M, Toniazzo V, Ruch D. Review of thermal conductivity in composites: Mechanisms, parameters and theory. Prog. Polym. Sci. 2016; 61: 1-28.

[3] Chen H, Ginzburg VV, Yang J, Yang Y, Liu W, Huang Y, Du L, Chen B. Thermal conductivity of polymer-based composites: Fundamentals and applications. Prog. Polym. Sci. 2016; 59: 41-85.

[4] Im H, Kim J. Thermal conductivity of a graphene oxide-carbon nanotube hybrid/epoxy composite. Carbon 2012; 50: 5429-5440.

[5] Huang X, Jiang P. A Review of dielectric polymer composites with high thermal conductivity. IEEE Electric. Insul. Mag. 2011; 27: 8-16.

[6] Donnay M, Tzavalas S, Logakis E. Boron nitride filled epoxy with improved thermal conductivity and dielectric breakdown strength. Compos Sci. Technol. 2015; 110: 152-158

[7] Yung KC, Zhu BL, Yue TM, Xie CS. Development of epoxy-matrix composite with both high-thermal conductivity and low-dielectric constant via hybrid filler system. J. Appl. Polym. Sci. 2010; 116: 518-527.

[8] Thermosets: Structure, properties and applications. Guo Q, editor. Woodhead Publishing Limited, 2012, Cambridge.

[9] Mir I, Kumar D. Recent advances in isotropic conductive adhesives for electronics packaging applications. Int. J. Adhes. Adhes. 2008; 28: 362–371.

[10] Gu H, Ma C, Gu J, Guo J, Yan X, Huang J, Zhang Q, Guo Z. An overview of multifunctional epoxy nanocomposites. J. Mater. Chem. C. 2016; 4: 5890-5906.

[11] Rybak A, Gaska K. Functional composites with core-shell fillers: I. Particle synthesis and thermal conductivity measurements. J. Mat. Sci. 2015; 50: 7779-7789.

[12] Yang K, Gu M. Enhanced thermal conductivity of epoxy nanocomposites filled with hybrid filler system of triethylenetetramine-functionalized multi-walled carbon nanotubes/silane-modified nano-sized silicon carbide. Composites: Part A 2010; 41: 215-221.

[13] Yu J, Mo H, Jiang P. Polymer/boron nitride nanosheet composite with high thermal conductivity and sufficient dielectric strength. Polym. Adv. Technol. 2015; 26: 514-520.

[14] Hou J, Li G, Yang N, Qin L, Grami ME, Zhang Q, Wang N, Qu X. Preparation and characterization of surface modified boron nitride epoxy composites with enhanced thermal conductivity. RSC Advances 2014; 4: 44282-44290.

[15] Pu X, Zhang H-B, Li X, Gui C, Yu Z-Z. Thermally conductive and electrically insulating epoxy nanocomposites with silica-coated graphene. RSC Advances 2014; 4: 15297–15303.

[16] Song SH, Park KH, Kim BH, Choi YW, Jun GH, Lee DJ, Kong B-S, Paik K-W, Jeon S. Enhanced Thermal Conductivity of Epoxy–Graphene Composites by Using Non-Oxidized Graphene Flakes with Non-Covalent Functionalization. Adv. Mater. 2013; 25: 732–737.

[17] Chatterjee S, Wang JW, Kuo WS, Tai NH, Salzmann C, Li WL, Hollertz R, Nüesch FA, Chu BTT. Mechanical reinforcement and thermal conductivity in expanded graphene nanoplatelets reinforced epoxy composites. Chem. Phys. Lett. 2012; 531: 6–10.

[18] Pashayi K, Fard HR, Lai F, Iruvanti S, Plawsky J, Borca-Tasciuc T. High thermal conductivity epoxy-silver composites based on self-constructed nanostructured metallic networks. J. Appl. Phys. 2012; 111: 104310.

[19] Xu Y, Chung DDL, Mroz C. Thermally conducting aluminium nitride polymer-matrix composites. Composites: Part A. 2001; 32: 1749-1757.

[20] Wang Z, Iizuka T, Kozako M, Ohki Y, Tanaka T. Development of epoxy/BN composites with high thermal conductivity and sufficient dielectric breakdown strength. Part I-Sample preparations and thermal conductivity. IEEE Trans. Dielectr. Electr. Insul. 2011; 18: 1963-1972.

[21] Vidil T, Tournilhac F, Musso S, Robisson A, Leibler L. Control of reactions and network structures of epoxy thermosets. Prog. Polym. Sci. 2016; 62: 126–179.

[22] Epoxy Polymers: New Materials and Innovations, Pascault JP, Williams RJJ, editors. Wiley-VCH, Weinheim, 2010.

[23] Nakano S, Endo T. Cationic polymerization of glycidyl phenyl ether by benzylammonium salts. J. Polym. Sci.: Part A: Polym. Chem. 1995; 33: 505-512.

[24] Nakano S, Endo T. Thermal cationic curing by benzylpyridinium salts. Prog. Org. Coat. 1994; 23: 379-385.

[25] Park S-J, Heo G-Y, Suh D-H. Thermal properties and fracture toughness of epoxy resins cured by phosphonium and pyrazinium salts as latent cationic initiators. J. Polym. Sci.: Part A: Polym. Chem. 2003; 41: 2393-2403.

[26] Jang ES, Khan SB, Seo J, Akhtar K, Nam YN, Seo KW, Han H. Preparation of cationic latent initiators containing imidazole group and their effects on the properties of DGEBA epoxy resin. Macromol. Res. 2011; 19 (10): 989-997.

[27] Toneri T, Watanabe K, Sanda F, Endo T. Synthesis and the initiator activity of fluorenyltriphenylphosphonium salts in the cationic polymerization of epoxide. Novel thermally latent initiators. Macromolecules, 1999; 32: 1293-1296.

[28] Endo T, Sanda F. Design of latent catalysts and their application to polymer synthesis. Macromol. Symp., 1996; 107: 237-242.

[29] Nakano S, Endo T. Thermal cationic curing with benzylammonium salts-2. Prog. Org. Coat. 1996 28: 143-148.

[30] Coats AW, Redfern JP. Kinetic Parameters from Thermogravimetric Data. Nature 1964; 201: 68-69.

[31] Ramis X, Salla JM, Mas C, Mantecón A, Serra A, Kinetic Study by FTIR, TMA, and DSC of the Curing of a Mixture of DGEBA Resin and γ-Butyrolactone Catalyzed by Ytterbium Triflate, J. Appl. Polym. Sci. 2004; 92: 381-393.

[32] Thermosetting Polymers, Pascault JP, Sauterau H, Verdu J, Williams RJJ, editors. Marcel Dekker, New York, 2002.

[33] Shugg WT. Handbook of electrical and electronic insulating materials. Van Nostrand Reinhold, New York, 1986.

[34] Ueki MM, Zanin M. Influence of additives on the dielectric strength of high-density polyethylene. IEEE Transactions on Dielectrics and Electrical Insulation 1999; 6: 876-881.

[35] Ross R. Graphical methods for plotting and evaluating Weibull distribution data. Proc. IEEE. 1994; 1: 250-253.

[36] Kubisa P, Penczeck S, Cationic activated monomer polymerization of heterocyclic monomers. Prog. Polym. Sci. 1999; 24: 1409-1437.

[37] Matejka L, Chabanne P, Tighzert L, Pascault JP. Cationic polymerization of diglycidyl ether of bisphenol A. J. Polym. Sci. Part A: Polym. Chem. 1994; 32: 1447-1458.

[38] Salla JM, Fernández-Francos X, Ramis X, Mas C, Mantecón A, Serra A. Influence of the proportion of ytterbium triflate as initiator on the mechanism of copolymerization of DGEBA epoxy resin and □-butyrolactone. J. Therm. Anal. Calorim. 2008; 91: 385-393.

[39] Arnebold A, Thiel K, Kentzinger E, Hartwig A. Morphological adjustment determines the properties of cationically polymerized epoxy resins. RSC Advances 2015; 54: 2482-42491.

[40] Biedron T, Szymanski R, Kubisa P, Penczek S, Kinetics of polymerization by activated monomer mechanism. Macromol. Chem. Macromol. Symp. 1990; 32: 155-168.

[41] Ivin KJ. Polymer Handbook. Brandrup J, Immergut EH, editors. Wiley, New York, 1975.

[42] Santiago D, Morell M, Fernández-Francos X, Serra A, Salla JM, Ramis X. Influence of the end groups of hyperbranched poly(glycidol) on the cationic curing and morphology of diglycidylether of bisfenol A thermosets. React. Funct. Polym. 2011; 71: 380–389.

[43] Yu J, Huang X, Wu C, Wu X, Wang G, Jiang P. Interfacial modification of boron nitride nanoplatelets for epoxy composites with improved thermal properties. Polymer 2012; 53: 471-480.

[44] Sato K, Horibe H, Shirai T, Hotta Y, Nakano H, Nagai H, Mitsuishi K, Watari K. Thermally conductive composite films of hexagonal boron nitride and polymide with affinity-enhanced interfaces. J. Mat. Chem. 2010; 20: 2749-2752.

[45] Vyazovkin S, Wight CA. Kinetic in Solids, Annu. Rev. Phys. Chem. 1997; 48: 125-149.

[46] Carreau PJ, De Kee DCR, Chhabra RP. Rheology of Polymeric Systems: Principles and Applications. Hanser Publishers, Munich, 1997.

[47] Han CD. Rheology and Processing of Polymeric Materials. Vol. 1. Oxford University Press, New York, 2007.

[48] Kamal MR, Mutel A. Rheological Properties of Suspensions in Newtonian and Non-Newtonian Fluids. J. Polym. Eng. 1985; 5: 293-382.

[49] Han C, Lem K. Rheology of unsaturated polyester resins. II. Thickening behavior of unsaturated polyester and vinyl ester resins. J. Appl. Polym. Sci. 1983; 28: 763-778.

[50] Ren J, Krishnamoorti R. Nonlinear Viscoelastic Properties of Layered-Silicate-Based Intercalated Nanocomposites. Macromolecules 2003; 36: 4443-4451.

[51] Macosko CW, RG Larson. Rheology: Principles, measurements, and applications. Wiley-VCH, New York, 1994.

[52] Tadros TF. Rheology of Dispersions: Principles and Applications. Wiley-VCH, Weinheim, 2010.

[53] Du F, Scogna RC, Zhou W, Brand S, Fisher JE, Winey KI. Nanotube Networks in Polymer Nanocomposites: Rheology and Electrical Conductivity. Macromolecules 2004; 37: 9048-9055.

[54] Hu G, Zhao C, Zhang S, Yang M, Wang Z. Low percolation thresholds of electrical conductivity and Rheology in poly(ethylene terephthalate) through the networks of multi-walled carbon nanotubes. Polymer 2006; 47: 480-488.

[55] De Gennes PG. Scaling theory of polymer adsorption. J. Phys. 1976; 37: 1445-1452.

[56] Feng S, Sen PN, Halperin BI, Lobb CJ. Percolation on two-dimensional elastic networks with rotationally invariant bond-bending forces. Phys. Rev. B. 1984; 30: 5386-5389.

[57] Flory PJ. Molecular size distribution in three dimensional polymers I. Gelation. J. Am. Chem. Soc. 1941; 63: 3083-3090.

[58] Dusek K, Duskova-Smrckova M, Network structure formation during crosslinking of organic coating systems. Prog. Polym. Sci. 2000; 25: 1215-1260.

[59] Ng H, Manas-Zloczower I. Chemorheology of unfilled and filled epoxy-resins. Polym. Eng. Sci. 1993; 33: 211-216.

[60] Becker O, Simon GP, Bailey RJ. Layered silicate nanocomposites based on various high functionality epoxy resins: The influence of an organoclay on resin cure. Polym. Eng. Sci. 2003; 43: 850-862.

[61] Yung C, Liem H. Enhanced thermal conductivity of boron nitride epoxy-matrix composite through multi-modal particle size mixing. J. Appl. Polym. Sci. 2007; 106: 3587-3591.

[62] Zhang Y. Adhesion of epoxy coatings to an alloy-coated steel sheet. Doctor of Philosophy Thesis. Department of Materials Engineering, University of Wollongong 1995 http:/ro.uow.edu.au/theses/1481. Access on March 23th 2017

[63] Fang L, Wu C, Quian R, Xie L, Yang K, Jiang P. Nano-micro structure of functionalized boron nitride and aluminium oxide for epoxy composites with enhanced thermal conductivity and breakdown strength. RSC Advances, 2014; 4: 21010-21017.

[64] Alam MT, Bresnehan MS, Robinson JA, Haque MA. Thermal conductivity of ultra-thin chemical vapor deposited hexagonal boron nitride films. Appl. Phys. Lett. 2014; 104: 13113-13118.